



Preparation and characterization of sodium cellulose sulfate/chitosan composite films loaded with curcumin for monitoring pork freshness

Chuan Tang^{a,b,*}, Zhixin Zhao^a, Ming Yang^a, Xuan Lu^a, Li Fu^b, Ge Jiang^{a,**}

^a College of Life Science and Technology, Dalian University, Dalian, Liaoning, 116622, China

^b Dalian Fusheng Natural Medicinal Development Co. Limited, Dalian, Liaoning, 116600, China

ARTICLE INFO

Handling Editor name: Dr. Xing Chen

Keywords:

Sodium cellulose sulfate
Chitosan
Curcumin
Pork preservation
Intelligent packaging

ABSTRACT

Colorimetric films were prepared by incorporating curcumin into a sodium cellulose sulfate/chitosan composite. The morphology mechanical, and water vapor properties of the films were investigated, and their practical use in pork preservation was evaluated. The formula with the same charge ratio of sodium cellulose sulfate and chitosan had the highest tensile strength (TS). After the addition of curcumin, the tensile strength increased, whereas the water vapor permeability (WVP) decreased. The colorimetric film showed distinguishable color changes between the pH ranges of 3–10. The colorimetric film packaging extended the shelf life of the pork samples by 4 days. Moreover, the composite films were able to effectively monitor pork freshness. In conclusion, curcumin incorporated into sodium cellulose sulfate/chitosan composite films may have great potential in food packaging.

1. Introduction

Meat spoilage not only causes great economic losses, but when consumed spoiled meat can seriously harms human health. For food safety assurance, real-time monitoring of meat freshness is essential for consumers and food manufacturing enterprises. An intelligent packaging system that can effectively monitor food quality without causing damage needs to be developed (Shao et al., 2021; Kang et al., 2020).

The internal environmental changes in food can be detected by using packaging that can monitor food quality. Colorimetric pH indicators have aroused the interest of researchers in food packaging (Zhang et al., 2019). The changes in pH that occur with food spoilage can be detected using a colorimetric pH indicator. Volatile amines are gradually released from decaying food, which causes an increase in the pH of the packaging. Curcumin (Cur) is a polyphenol extracted from turmeric, an herb, and its rhizomes. It has anti-inflammatory, antioxidant, anticancer, antibacterial, and pH-responsive properties (Liu et al., 2018). Due to its indicator properties, curcumin has a high potential to be used for intelligent packaging (Roy and Rhim, 2020).

The solid matrix, which is used to immobilize colorimetric pH indicators, plays an important role in food packaging. It must be safe, sensitive, and environmentally sustainable. Traditional food packaging

is mainly made of plastic products, such as polyethylene, which causes great environmental damage (Pirsa et al., 2020; Akyuz et al., 2017; Kalkan et al., 2020). In particular, there has been increasing concern regarding the negative environmental impacts of petroleum-derived plastic packaging materials. Therefore, naturally degradable biomaterials have aroused great interest in academia and industry (Zhu et al., 2019; Medina-Jaramillo et al., 2017).

Cellulose is an inexhaustible material, and of all natural polymers, it is the most valuable naturally renewable polymer. It exists in the form of a simple polysaccharide without any substituents or branches. Hence, it is easier to modify or derivatize its structure (Wu et al., 2018). Various derivatives with different degrees of substitution can be obtained by the reaction of hydroxyl groups with chemical reagents, such as esters and ethers. Owing to their various biological properties, these derivatives have several applications in food, medical, and pharmaceutical industries (Zhang et al., 2015). Sodium cellulose sulfate (NaCS) is derived from cellulose, and it contains $-SO_3$ as the active group. It is biocompatible, biodegradable, water-soluble, and has excellent film-forming, antiviral, anticoagulative, and antimicrobial properties (Chen et al., 2013; Muhitdinov et al., 2017; Scordi-Bello et al., 2005; Wang et al., 2007). However, only a few studies on food packaging made of NaCS have been reported (Chen et al., 2014a, b). Chen et al. (2014a) prepared

* Corresponding author. College of Life Science and Technology, Dalian University, Dalian, Liaoning, 116622, China.

** Corresponding author.

E-mail addresses: jiemotc@gmail.com (C. Tang), jiangge1004@163.com (G. Jiang).

<https://doi.org/10.1016/j.crfs.2022.08.019>

Received 27 May 2022; Received in revised form 14 August 2022; Accepted 26 August 2022

Available online 8 September 2022

2665-9271/© 2022 The Authors. Published by Elsevier B.V. This is an open access article under the CC BY-NC-ND license (<http://creativecommons.org/licenses/by-nc-nd/4.0/>).

NaCS films blended with cassava starch for use in edible packaging. They reported that adding a small amount of cassava starch increased the hydrophobicity of the NaCS films without reducing their mechanical properties and water vapor permeability (WVP). Furthermore, edible cellulose sulfate-based films were also prepared (Chen et al. 2014b) and it was reported that increasing the molecular weight of cellulose sulfate (CS) improved the tensile strength (TS) and elongation at break (EAB), whereas the addition of glycerol decreased the TS. In addition, WVP decreased with the addition of glycerol, and the molecular weight of CS increased. These studies mainly focused on the mechanical properties and WVP of the NaCS based films, the investigation on properties towards packaging applications, such as antibacterial activity, preservation ability, and freshness indication ability were absent. Chitosan (CH) is a partially N-deacetylated derivative of chitin, which mostly exists in marine crustaceans, such as shrimp and crabs, insects, fungi, and algal cell membranes (Zimet et al., 2019). It is less toxic, biocompatible, completely biodegradable, and has excellent film-forming properties. Based on these properties, it has become a potential candidate in active food packaging (Kadam et al., 2019). As a natural polycationic polysaccharide, CH can be electrostatically combined with other anionic compounds, such as NaCS, to form polyelectrolyte complexes with improved physical properties. NaCS/CH polyelectrolyte composite films have long been reported as drug carriers for controlled oral release (Zhu et al., 2010) and as potential materials for colon-specific drug delivery systems (Wang et al., 2010). Using a layer-by-layer method, CH and cellulose sulfate films have also been prepared for cell culturing (Aggarwal et al., 2013).

Therefore, biodegradable, low-toxicity, and low-cost intelligent packaging based on NaCS and CH mixtures are highly desirable. However, there is a dearth in published studies on their development for food packaging. In the present study, a novel NaCS and CH-based food packaging loaded with curcumin was developed to monitor and maintain the freshness of pork. The color change of curcumin along with pH change was studied, and the effect of different polymer formulations on the mechanical properties of the composite films was investigated. Finally, the colorimetric films were used to monitor the freshness of pork at the refrigeration temperature (4 °C).

2. Materials and methods

2.1. Materials

The pork was purchased from a local market in Liaoning, China. Chitosan (degree of deacetylation, 85%) was purchased from Jinan Haidebei Marine Bioengineering Co., China. NaCS (degree of substitution 0.8) was prepared using a previously reported method (Chen et al., 2013). Trichloroacetic acid (TCA), curcumin, and glycerol (analytical grade) were purchased from Sinopharm Chemical Reagent Co., Ltd., China. LB broth and all-purpose agar were purchased from Sangon Biotech Co. Ltd. (Shanghai, China). Sodium hydroxide (NaOH), malondialdehyde (MDA), thiobarbituric acid (TBA), acetic acid, ethanol, disodium hydrogen phosphate (Na₂HPO₄), magnesium oxide (MgO), hydrochloric acid (HCl), boric acid (H₃BO₃), anhydrous calcium chloride (CaCl₂), methylene blue, and methyl red were purchased from Kermel Chemical Reagent Co. Ltd., China. Polyethylene (PE) plastic wrap was purchased from Shenke Household Products Co., Ltd., China.

2.2. Preparation of the composite films

The composite films were prepared using an electrostatic self-assembly technique. The film-forming solution was prepared as follows. First, NaCS was dissolved in distilled water and CH was dissolved in 1% v/v acetic acid to prepare 1% w/v NaCS and 1% w/v CH solutions. Different electrostatic forces affect the properties of composite films. Based on the degree of substitution of NaCS and the degree of deacetylation of CH, five groups of films with different charge ratios, 2:0, 2:1,

2:2, 1:2, and 0:2, were selected for this study. The film-forming solution was mixed and stirred for 1 h after the addition of 0.5% glycerol (v/v film-forming solution). Finally, the film-forming solution was cast on a Teflon mold (10 cm × 10 cm) after vacuum degasification and dried for 24 h at 40 °C on a heating plate. The dried films were peeled out from the Teflon mold, vacuum sealed, and stored in a refrigerator (below 4 °C) for further use. The films with charge ratios 2:0, 2:1, 2:2, 1:2, and 0:2 were denoted as NaCS/CH2:0, NaCS/CH2:1, NaCS/CH2:2, NaCS/CH1:2, and NaCS/CH0:2, respectively. Colorimetric films were prepared based on NaCS/CH2:2 loaded with curcumin, namely NaCS/CH/Cur. To fabricate colorimetric films loaded with curcumin, curcumin was dissolved in 5 mL ethanol to prepare the curcumin solution. Subsequently, the curcumin solution and film-forming solution were mixed and stirred evenly. Subsequently, the film-forming solution was cast on a Teflon mold and allowed to dry to form a colorimetric film containing 6 wt% curcumin. The colorimetric film was denoted as NaCS/CH/Cur.

2.3. UV-vis spectroscopy analysis of curcumin solution

The ultraviolet-visible (UV-vis) spectra of curcumin were measured using a UV-vis spectrophotometer (JASCO-V560, JASCO, Japan) in the range of 250–700 nm. Curcumin was dissolved in a phosphate buffer solution at pH 3.0–10.0, and a buffer solution without curcumin was used as blank.

2.4. Characterization and properties of composite films

2.4.1. Thickness and mechanical properties

A micrometer caliper (Mitutoyo, Mizonokuchi, Japan) with a precision of 1 μm was used to measure the thicknesses of the sample films. Five positions were randomly selected on the film, and the mean value was calculated as the final result. Each sample was measured five times.

Using the method described by Zhang et al. (2019), a tensile testing machine (Model 506, Dongri Instruments, China) was used to measure TS and EB in accordance with ASTM D882. The sample films were cut into rectangles with dimensions of 2 cm × 10 cm and stretched at a speed of 5 mm/min until breakage. Each sample was measured five times.

2.4.2. Water vapor permeability (WVP)

The method used for measuring the WVP of the composite films was adapted from a previous study (Huang et al., 2020). Calcium chloride (3.0 g) was placed in a permeation cup that was tightly sealed with a film. The permeation cup was maintained at 75% for 48 h. The permeation cup was weighed once every 1 h.

$$WVP = (\Delta m \times d) / (S \times \Delta P \times t) \quad (1)$$

where Δm is the change in weight of the permeation cup, d is the mean thickness of the sample, ΔP is the pressure difference on both sides of the film, t is the permeation time, and S is the exposed area of the film. Each sample was measured thrice.

2.4.3. Fourier-transform infrared analysis

A Fourier transform infrared (FTIR) spectrophotometer (Nicolet550 FT-IR Spectrometer, Thermo Nicolet Corporation, USA) was used to determine the FTIR spectra of the films. For each spectrum, 32 scans were captured between 4000 and 500 cm⁻¹ with a resolution of 4 cm⁻¹.

2.4.4. Film morphology

The microstructures of the films were observed using scanning electron microscopy (SEM) (S-4800 Hitachi, Tokyo, Japan). Each film sample was sprayed with a thin layer of gold using a vacuum sputter coater for 30 s, and the microstructure was observed.

2.4.5. X-ray diffraction (XRD) spectroscopy

X-ray diffraction (XRD) patterns of the films were obtained by an X-ray diffractometer (Rigaku, Japan) equipped with Ni-filtered Cu K α radiation ($\lambda = 1.5418$ nm). Diffraction curves were collected in the region of 5–60° (2 θ) at 2°/min speed.

2.4.6. Color response analysis

In order to investigate the response of the films to different pH values, they were placed in a buffer solution with pH in the range of 3–10, and the color changes were measured using a colorimeter (WR-10, Shenzhen Weifu Photoelectric Technology Co., Ltd, China) and photographed. Each sample was analyzed thrice. The total color difference (ΔE) was calculated as follows:

$$\Delta E = \sqrt{(L^* - L_0^*)^2 + (a^* - a_0^*)^2 + (b^* - b_0^*)^2} \quad (2)$$

where L^* , a^* , and b^* are the color parameters of lightness, chromaticity index (positive express red and negative express green), and chromaticity index (positive express yellow and negative express blue), respectively. L_0^* , a_0^* , and b_0^* are the color parameters of the white paper background ($L_0^* = 88.14$, $a_0^* = -1.81$, $b_0^* = -0.56$).

2.5. Preservation of pork and monitoring of pork spoilage

2.5.1. Processing of pork

The pork test sample (10.0 g) was wrapped in a colorimetric film, and pork wrapped in polyethylene (PE) plastic and uncoated pork of the same weight were set as control and blank control, respectively. All the samples were placed in sterilized Petri dishes (diameter 9 cm) separately in a refrigerator at 4 °C for 10 days. The pH, total volatile basic nitrogen (TVB-N), total viable count (TVC), and thiobarbituric acid reactive substances (TBARS) of the samples were measured every 2 days.

2.5.2. Determination of pH, TVB-N, TVC, and TBARS contents

To investigate the pH change in pork during storage, the samples were removed from the refrigerator at 4 °C after a specific time interval, minced, and mixed with 100 mL deionized water, and stirred. The samples were then allowed to settle for 30 min. Finally, the samples were measured using a pH meter (FE20; Mettler Toledo, USA). Each experiment was performed in triplicate.

The freshness of pork can be determined by measuring TVB-N levels. The semi-micro Kjeldahl method for measuring TVB-N content (Sun et al., 2020) was adopted. A mixture of MgO suspension (10 g/L) and pork samples was distilled. Distillation was performed using a boric acid solution (20 g/L) containing a mixed indicator. The indicator was prepared using methyl red and methylene blue. The boric acid solution was titrated with HCl solution (0.365 g/L) until it turned pink. The results are expressed in mg/100 g. Each experiment was performed in triplicate.

TVC is another index that determines the freshness of pork. The TVC content of the sample was measured using the plate colony counting method (Kim et al., 2017) and expressed in Log (CFU/g). On each sampling day, 10 g of the sample was aseptically transferred to a 100 mL sterile bag, and 90 mL of sterile LB liquid medium was added. Serial decimal dilutions using LB liquid medium were prepared, and 1.0 mL samples at appropriate dilution ratios were poured on all-purpose LB agar plates. The plates were incubated at 37 °C for 48 h. The microbial count was determined in triplicate using a bacterial colony counter (XK97-A, Hangzhou Qiwei Instrument Co., Ltd., China). Each experiment was performed in triplicate.

One of the most commonly used methods for monitoring the secondary products of lipid oxidation, TBARS, can reflect the degree of fat oxidation. The TBARS content of the samples was measured using a spectrophotometric method (Medić et al., 2018) and expressed in mg MDA/kg. A standard curve of malondialdehyde (MDA) was generated. The pork sample (5 g) was homogenized thrice for 20 s with a homogenizer (FJ200, Shanghai Hushi Industrial Co., Ltd, China) in 7.5% TCA

solution (50 mL). The filtrate (5 mL) and the same volume of 0.02 M TBA solution were mixed. Next, the mixed solution was heated in a water bath at 40 °C for 100 min. After cooling, the absorbance was read at 538 nm using a spectrophotometer (WR-10, GASCO, Japan). The MDA content was determined according to the standard curve. Each experiment was performed in triplicate.

2.6. Statistical analysis

All data are expressed as mean \pm standard deviation after analysis using SPSS 21.0. Duncan's multiple range test ($p < 0.05$) was used to determine the differences between the films.

3. Results and discussion

3.1. UV-vis spectra analysis

To validate curcumin as a pH indicator, color variations were tested in curcumin solutions at different pH values. As shown in Fig. 1A, the color of curcumin solutions was yellow at pH < 8, reddish orange at pH 8, and reddish brown at pH 9–10. These differences in the color of the solution can be attributed to the reversible transformation of the structure of curcumin at different pH values, and a schematic illustration is shown in Fig. 1B (Liu et al., 2018). As the alkalinity increased to pH 9, curcumin decomposed to more into ferulic acid and ferulic acid methane. A reddish-brown condensate formed rapidly by the combination of ferulic acid and ferulic acid methane (Wang et al., 1997). Fig. 1C shows the UV-vis spectra of the curcumin solutions at different pH values. The different profiles of the absorption spectra are displayed with the changes in pH. Under acidic conditions, the maximum absorption peak of curcumin solutions was around 429 nm. This phenomenon was attributed to the presence of phenolic compounds and unsaturated bonds and electron excitation from the π - π^* transition of curcumin. The maximum absorption wavelength of curcumin shifted from 429 nm to 444 nm due to the increase in pH. Similarly, the intensity of the peak increased gradually with increasing alkalinity. These results were also similar to previous reports (Chen et al., 2020).

3.2. Characterization and properties of composite films

3.2.1. Thickness and mechanical properties

The thicknesses, TS, and EB of the composite films are listed in Table 1. NaCS/CH composite films have lower thicknesses than pure NaCS film and pure CH film. This was probably because the hydrogen bond between NaCS and CH could enhance the tightness between NaCS molecules and CH molecules (Zhao et al., 2022). The TS and EB values of Control NaCS film were 0.65 MPa and 7.20%, respectively, which were lower compared with those reported by Chen (Chen et al., 2014). This may be due to the lower polymer and glycerol contents. Similar conclusion can be drawn from the study of Kurek and colleagues, who prepared CH film with higher TS and EB (Kurek et al., 2018). The mechanical properties of the composite films varied with the polymer ratio. The results showed that the tensile strength of the pure NaCS film was significantly ($p < 0.05$) lower than that of the composite films. The pure CS film had a lower tensile strength than NaCS/CH1:2 and NaCS/CH2:2. The highest TS value was observed for NaCS/CH2:2. This can be attributed to the electrostatic combination of the positively charged CH and the negatively charged NaCS to form a polyelectrolyte complex. NaCS/CH2:2 showed the strongest electrostatic force between its components and the highest TS, which are conducive for the integrity of the film matrix. We added curcumin to the NaCS/CH2:2-based composite films and measured their mechanical properties. The results showed that the mechanical properties of the composite films changed with curcumin addition. The TS of the NaCS/CH/Cur film was significantly ($p < 0.05$) higher than that of NaCS/CH2:2. This may be due to the uniform dispersion of curcumin in the polymer matrix, which forms a hydrogen

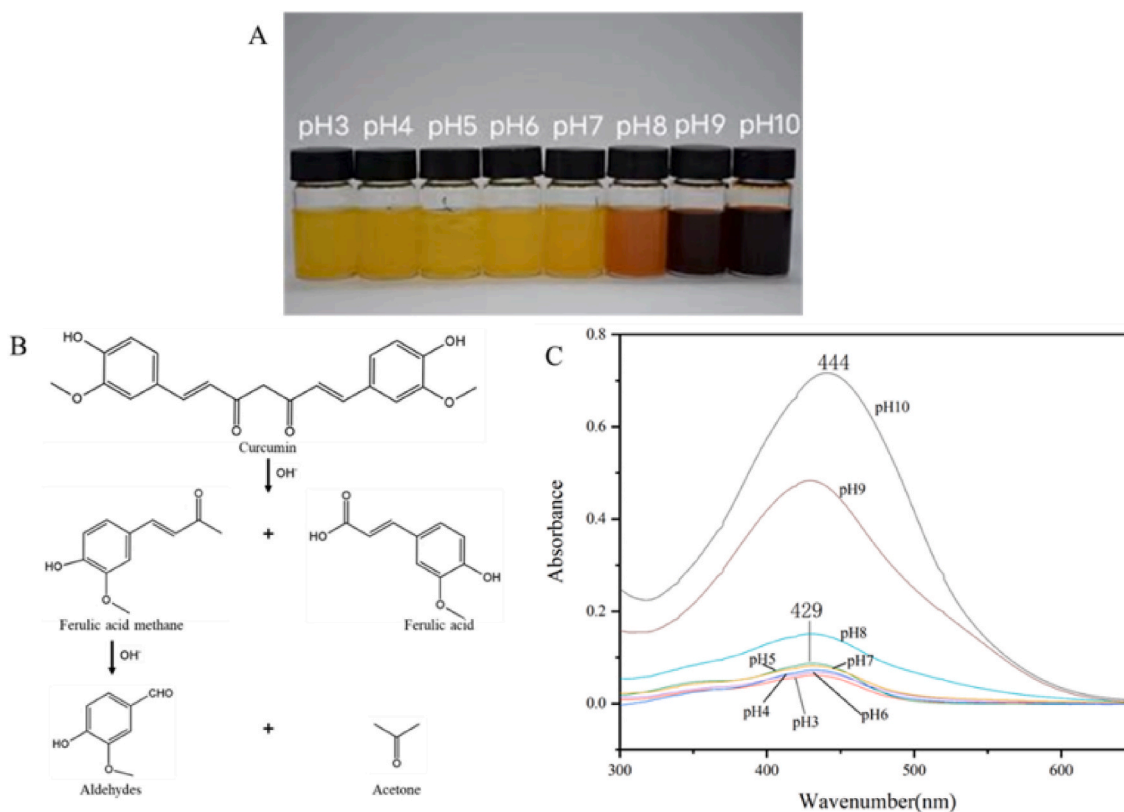


Fig. 1. (A) Photographs of curcumin solutions at different pH values; (B) Curcumin degrades in alkaline conditions; (C) UV-vis spectra of curcumin solutions at different pH values.

Table 1

The thickness, mechanical and barrier properties of the composite films.

Films	Thickness (μm)	TS (MPa)	EB (%)	WVP ($10^{-11} \text{gm}^{-1} \text{s}^{-1} \text{Pa}^{-1}$)
NaCS/CH2:0	84.60 \pm 4.67 ^a	0.65 \pm 0.13 ^c	7.20 \pm 2.77 ^d	9.25 \pm 0.28 ^b
NaCS/CH2:1	79.80 \pm 3.11 ^b	5.12 \pm 0.36 ^d	33.43 \pm 4.09 ^{bc}	9.72 \pm 0.16 ^{bc}
NaCS/CH2:2	79.20 \pm 1.92 ^b	8.17 \pm 0.70 ^b	42.28 \pm 1.20 ^{ab}	9.93 \pm 0.18 ^c
NaCS/CH1:2	78.40 \pm 1.52 ^b	7.35 \pm 0.62 ^b	47.81 \pm 2.71 ^a	9.30 \pm 0.14 ^b
NaCS/CH0:2	87.00 \pm 3.74 ^a	6.25 \pm 0.39 ^c	47.74 \pm 9.58 ^a	8.71 \pm 0.05 ^a
NaCS/CH/Cur	81.07 \pm 1.87 ^b	10.99 \pm 0.50 ^a	29.86 \pm 5.70 ^c	8.61 \pm 0.56 ^a

Means in the same column with different letters are statistically different ($p < 0.05$).

bond (Roy and Rhim, 2020; Pereda et al., 2011). NaCS/CH/Cur had a significantly lower EB than NaCS/CH2:2, and this was because of the rigid nature of curcumin, which restrained the motion of the polymer chains and caused decreased suppleness. A similar phenomenon was observed in previous studies on other composite films containing curcumin (Liu et al., 2018, 2022). Besides, the hydrophobic property of curcumin decreases the hydrophilicity of film, which increases TS and decreases EB (Pirsa et al., 2020; Riaz et al., 2020).

3.2.2. Water vapor permeability (WVP)

WVP is an essential parameter that determines the moisture transport ability of packaging films. Generally, food preservation requires an appropriate WVP. As shown in Table 1, the WVP of NaCS/CH0:2 was lower than that of the other films without curcumin. In contrast,

previous studies reported that starch has better barrier properties against water vapor than CH (Chen et al., 2013). With increasing level of NaCS, the WVP of the composite films increased significantly ($p < 0.05$), and NaCS/CH2:2 had the highest WVP. The barrier ability of NaCS/CH2:2 to water vapor was slightly weaker than that of the other films, which is not conducive for food preservation. The increase in the WVP of NaCS/CH2:2 may be due to the influence of electrostatic force, which led to the formation of tomograph in the matrix (Liu et al., 2020). The uniformity of the film was destroyed, resulting in easier passage of water vapor. However, the WVP of NaCS/CH/Cur decreased significantly ($p < 0.05$), compared with that of NaCS/CH2:2, which can be attributed to the hydrophobic nature of curcumin. Similarly, a decrease in WVP was observed in CH films loaded with hydrophobic fillers (Ezati and Rhim, 2020). This may also be attributed to the hydrogen and covalent interactions between the matrix network and polyphenolic compounds, which reduced the availability of hydrophilic groups and led to a subsequent decrease in the affinity of the NaCS/CH/Cur film for water molecules. Similar findings were observed by Kurek, who found that the interactions between CH and blueberry extracts increased when the extracts were incorporated into the matrix. This led to a decrease in the diffusivity of water vapor through the film matrix and a decrease in their hydrophilicity (Kurek et al., 2018).

3.2.3. FTIR analysis

The molecular interactions within the composite films were analyzed using FT-IR spectroscopy, and the results are shown in Fig. 2. The characteristic peaks of NaCS observed at 1224 cm^{-1} and 815 cm^{-1} corresponded to the S=O and C–O–S groups, respectively (Chen et al., 2013). The absorption peak at 3426 cm^{-1} was ascribed to the OH stretching vibration. The FT-IR spectrum of CH exhibited peaks at 3409 cm^{-1} (O–H stretching), 1650 cm^{-1} (C=O stretching), and 1594 cm^{-1} (N–H bending). After preparing the composite films, the CH peak at 3409 cm^{-1} (O–H stretching) shifted to 3394–3378 cm^{-1} , which could

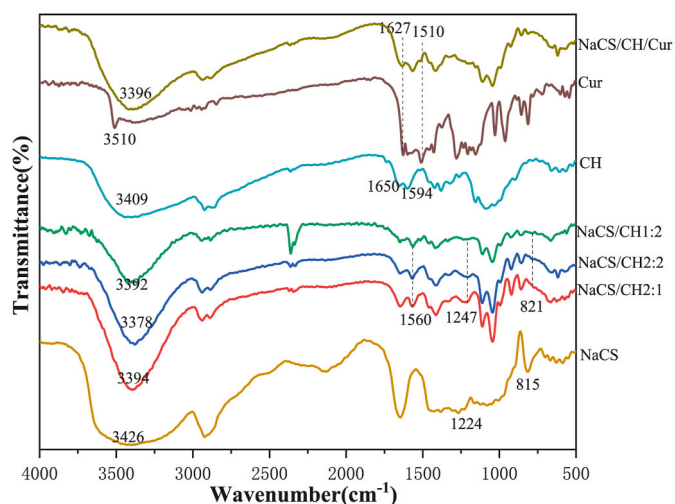


Fig. 2. FTIR spectra of NaCS/CH2:1, NaCS/CH2:2, NaCS/CH1:2, NaCS, CH, Curcumin and NaCS/CH/Cur colorimetric film.

be attributed to the hydrogen bonds between CS and NaCS (Chen et al., 2018). The formation of hydrogen bonds reduced the force constant of chemical bonds, then the absorption frequency shifted to the low wave number direction. In addition, the peak of CH at 1594 cm^{-1} (N–H bending of CH) shifted to 1560 cm^{-1} , while that of NaCS at 1224 cm^{-1} (S=O stretching) and 815 cm^{-1} (C–O–S group) shifted to 1247 cm^{-1} and 821 cm^{-1} , respectively, which indicated that -NH^{3+} in CS and -SO^{3-} in NaCS electrostatically combined to form a polyelectrolyte complex (Su et al., 2019). The characteristic peak of curcumin at 3510 cm^{-1} was attributed to the O–H stretching vibration. The peak shifted in the spectrum of the NaCS/CH/Cur colorimetric film, indicating that curcumin may interact with CH or NaCS. The peaks at 1627 cm^{-1} and 1510 cm^{-1} were assigned to curcumin aromatic C=C stretching. These peaks also appeared in the spectra of the NaCS/CH/Cur colorimetric film. This confirmed that the appearance of the peaks at 1627 cm^{-1} and 1510 cm^{-1} was due to the presence of curcumin in the NaCS/CH/Cur colorimetric film (Yang et al., 2020).

3.2.4. Film morphology

The SEM images of the films are shown in Fig. 3. The NaCS/CH0:2 (Fig. 3A) and NaCS/CH0:2 (Fig. 3E) films showed relatively compact

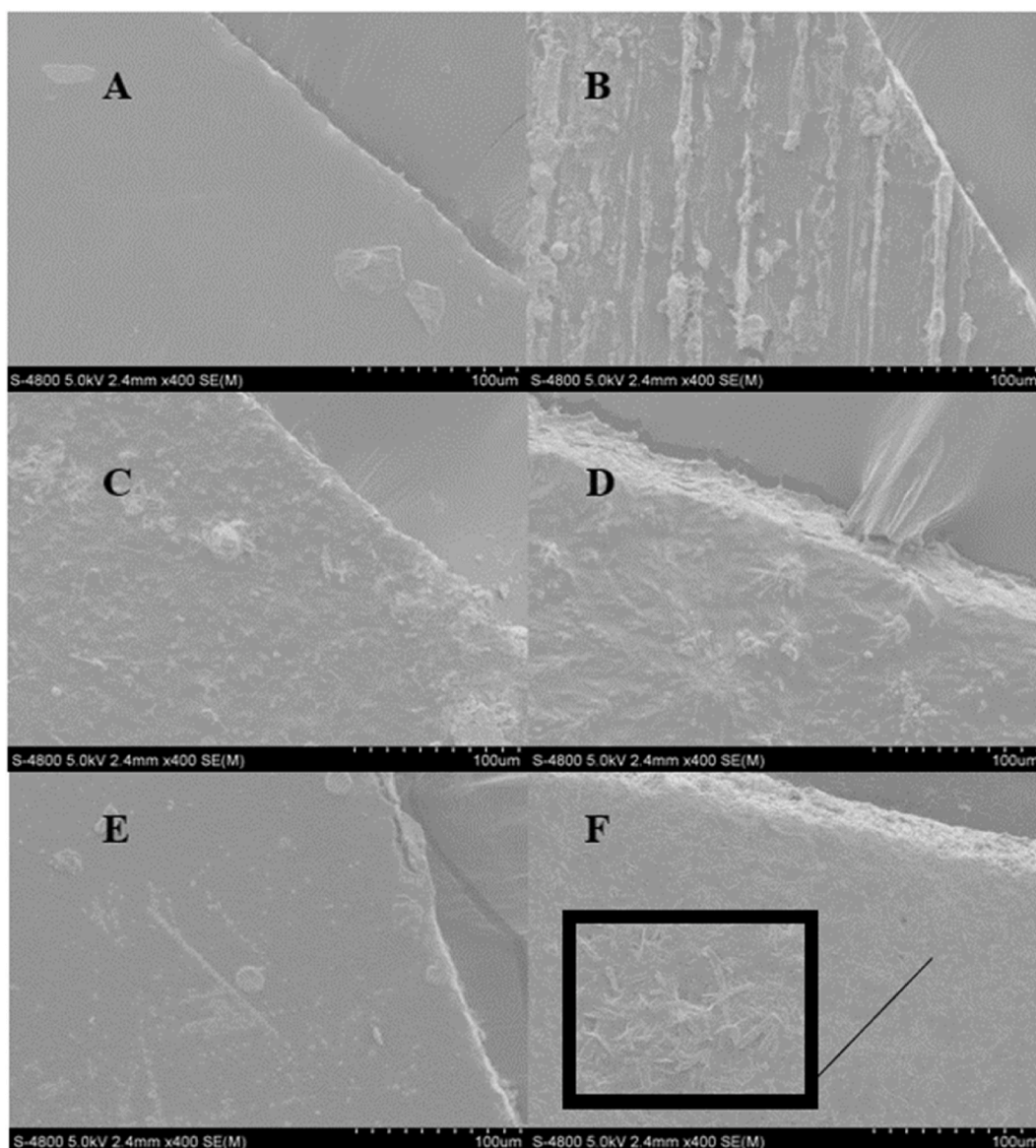


Fig. 3. SEM images of composite films. (A)NaCS/CH0:2. (B)NaCS/CH1:2. (C)NaCS/CH2:2. (D)NaCS/CH2:1. (E)NaCS/CH2:0. (F)NaCS/CH/Cur.

and smooth surfaces, indicating that CH and NaCS have excellent film-forming properties. These results are in agreement with those of previous studies (Pirsa et al., 2020; Chen^a et al., 2014). A rough surface was clearly observed on the NaCS/CH1:2 (Fig. 3B), NaCS/CH2:2 (Fig. 3C), and NaCS/CH2:1 films (Fig. 3D). This polyelectrolyte complex is formed by the electrostatic combination of CH and NaCS. As shown in Fig. 3F, the composite films loaded with curcumin showed a more homogeneous surface, and small precipitations and wrinkles were observed on the surface of the composite film, indicating that curcumin was successfully incorporated into the NaCS/CH film (Liu et al., 2018). Similar small precipitates and wrinkles were found in films prepared using agar incorporated with which natural dyes, and this was attributed to the agglomeration of the filler (Huang et al., 2019). A more compact and smoother surface was observed when natural dye was added to the polymer matrix, which was attributed to intermolecular associations established by hydrogen bonds (Yoshida et al., 2014; Zhai et al., 2017). The presence of curcumin facilitated the homogeneous mixing of NaCS and CH in the film. This was because the original molecular interactions between NaCS and CH were broken by new electrostatic interactions and hydrogen bonds (Wu et al., 2019), thereby reducing the roughness of the film surface.

3.2.5. XRD analysis

XRD patterns of CH, NaCS, Cur, NaCS/CH film and NaCS/CH/Cur film were shown in Fig. 4. The pure CH film exhibited a major characteristic peak at $2\theta = 19.8$, indicating amorphous structure of CH films (Wu et al., 2019). The appearance of a serial of 2θ diffraction angles at $7\text{--}30^\circ$ confirmed the crystalline structure of Cur (Liu et al., 2018). The diffraction peak intensity of NaCS/CH film was obviously lower than that of CH film and NaCS film. The reduction in crystallinity might be attributed to amorphous complexes formed through electrostatic force between NaCS and CH. The pattern of NaCS/CH/Cur films showed some weak diffraction peaks of Cur, indicating that the incorporated Cur was partially in crystalline form which was in consistent with the SEM observations.

3.2.6. Color response analysis

To evaluate the color response ability of the films, the NaCS/CH/Cur composite films were immersed in buffer solutions with pH in the range of 3.0–10.0. The color changes of the films to the changing pH differed slightly from the curcumin solution due to the effect of the polymer matrix. However, the main changes in color tint were similar. Table 2 shows the parameters of color changes. At pH 3.0–7.0, the films were yellow, which is due to higher value of b^* . A sudden change in the value

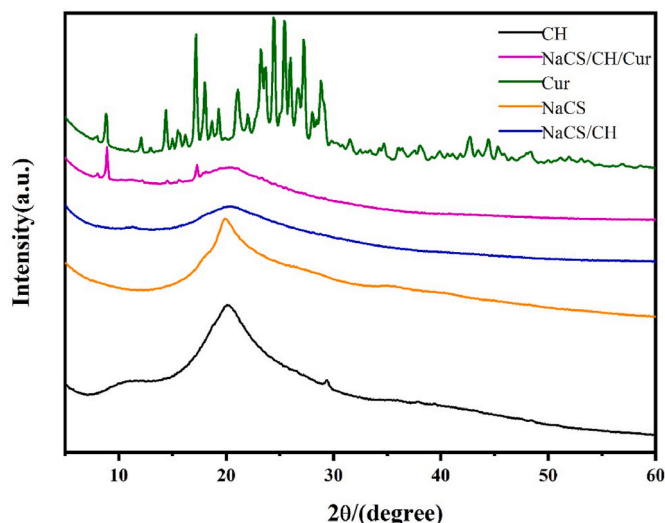


Fig. 4. XRD patterns of CH, NaCS, Cur and the NaCS/CH/Cur film.

Table 2

Color response of NaCS/CH/Cur film at different pH values.

pH	Photo	L*	a*	b*	ΔE
3		61.46 ± 0.74 ^f	28.36 ± 0.19 ^f	58.31 ± 0.63 ^d	71.34 ± 0.55 ^b
4		58.59 ± 0.27 ^{de}	27.42 ± 0.10 ^e	62.28 ± 0.76 ^d	75.35 ± 0.66 ^d
5		57.94 ± 1.23 ^d	29.55 ± 0.35 ^d	64.35 ± 0.82 ^f	78.17 ± 1.10 ^f
6		59.93 ± 0.03 ^c	29.52 ± 0.09 ^d	68.94 ± 0.05 ^e	81.28 ± 0.09 ^e
7		59.28 ± 1.64 ^{de}	31.37 ± 0.40 ^c	74.61 ± 0.58 ^h	87.10 ± 0.13 ^h
8		51.52 ± 0.26 ^b	35.75 ± 0.39 ^b	55.32 ± 1.13 ^c	76.65 ± 0.55 ^c
9		46.93 ± 0.26 ^b	35.78 ± 0.50 ^b	45.69 ± 0.55 ^b	72.46 ± 0.67 ^c
10		45.32 ± 0.34 ^a	36.76 ± 0.14 ^a	35.18 ± 0.89 ^a	67.82 ± 0.63 ^a

Means in the same column with different letters are statistically different ($p < 0.05$).

of b^* from 74.61 to 55.32 was detected in the buffer solution as the pH changed from 7 to 8, indicating a strong reduction of yellowness. Redness was significantly ($p < 0.05$) enhanced with an increase in alkalinity. The value of a^* changed from 31.37 to 35.75. Furthermore, with an increase in pH from 3 to 10, a significant ($p < 0.05$) change in ΔE from 71.34 to 67.82 allowed the color changes to be easily distinguished in plain sight. Liu et al. prepared a colorimetric film based on κ -carrageenan incorporated into curcumin. A similar color change in the composite was observed in solutions with different pH values (Liu et al., 2018) and in curcumin-loaded pectin films (Ezati and Rhim, 2019). The color changed from yellow under acidic conditions to red at pH 8 and then turned reddish-brown with increasing pH. This result suggests that the NaCS/CH/Cur composite films could effectively monitor changes in pH. These color changes were attributed to the transformation of curcumin (Fig. 1B).

3.3. Application in food packaging

To test the application of the colorimetric films in food packaging, NaCS/CH/Cur films were used to pack pork. The pH, TVB-N levels of the pork, and color parameters of the films were measured.

As shown in Fig. 5, after storage for 2 days, the pH of pork in the

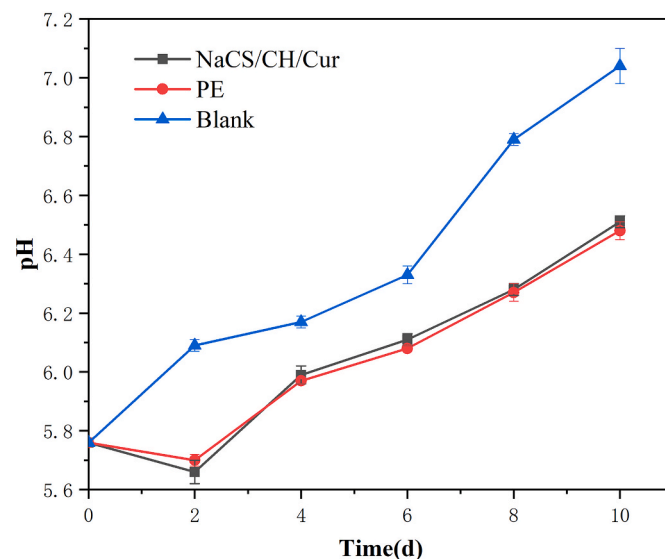


Fig. 5. Changes of pH of pork. (NaCS/CH/Cur: wrapped pork with colorimetric film; PE: wrapped pork with polyethylene film; Blank: uncoated pork).

NaCS/CH/Cur and PE groups decreased slightly. However, as protein degradation progressed, alkaline amines were generated and the pH level increased.

As shown in Fig. 6, on the second day, the TVB-N levels in the PE and NaCS/CH/Cur groups decreased. This was because there was a period of rigidity preceding pork spoilage. Lactic acid and phosphoric acid were produced during this time through muscle glycogen anaerobic glycolysis and adenosine triphosphate decomposition, which influenced the levels of TVB-N. These results are similar to a previous report (Yong et al., 2019). In the blank control group, the pH and TVB-N levels increased at the beginning of storage. This was possibly because pork was in contact with air, which reduced the production of acidic substances. During the initial 4 days, TVB-N value of the experimental group increased from 8.53 to 11.2 mg/100 g and then to 18.67 mg/100 g on the 6th day. According to the Chinese Standard (GB 2707-2016), the limit of the TVB-N value for pork is 15 mg/100 g. This suggests that the pork sample spoiled after 6 days. During the initial 4 days, TVB-N value of the PE control group increased from 8.53 to 11.67 mg/100 g and then to 20.07 mg/100 g on the 6th day. During the initial 2 days, the TVB-N value of the blank control group increased from 8.53 to 16.1 mg/100 g, and the results showed that the pork samples without food packaging spoiled within 2 days. Comparing these three groups, the results showed that the NaCS/CH/Cur film could extend the freshness of pork by 4 days.

As shown in Fig. 7, the TVC value of the experimental group was lower than those of the other groups on each sampling day. According to the China Agricultural Industry Standard (NY5029-2008), the limit of the TVC value for pork is 10^6 CFU/g (Editorial Department of agricultural standards, 2015). The pork-coated composite films were spoiled by the sixth day. Pork with PE and pork in the blank control were spoiled by the fourth day. These results showed that the NaCS/CH/Cur film inhibited bacterial growth in pork, indicating that curcumin confers its antibacterial properties on the NaCS/CH/Cur composite films (Roy and Rhim, 2020). The antibacterial property of curcumin involves the interference of the FtsZ protein required for cell proliferation and destruction of cell membrane potential (Kaur et al., 2010).

Fig. 8 shows the increase in the TBARS value of pork. The initial TBARS value was 0.188 mg/kg. The TBARS value of pork in each group continued to increase with increasing storage time. We noticed that the TBARS value of pork in the blank control was significantly higher than those in the other two groups during the storage process, indicating that the degree of lipid oxidation of pork in the NaCS/CH/Cur and PE groups

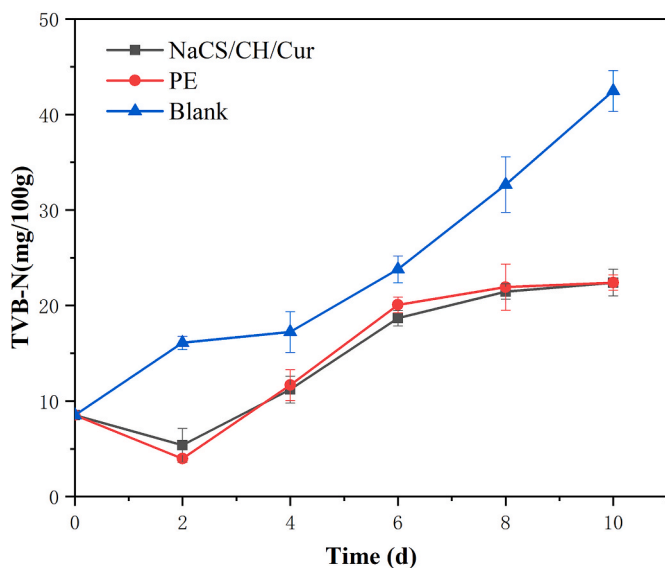


Fig. 6. Changes of total volatile basic nitrogen (TVB-N) levels of pork. (NaCS/CH/Cur: wrapped pork with colorimetric film; PE: wrapped pork with polyethylene film; Blank: uncoated pork).

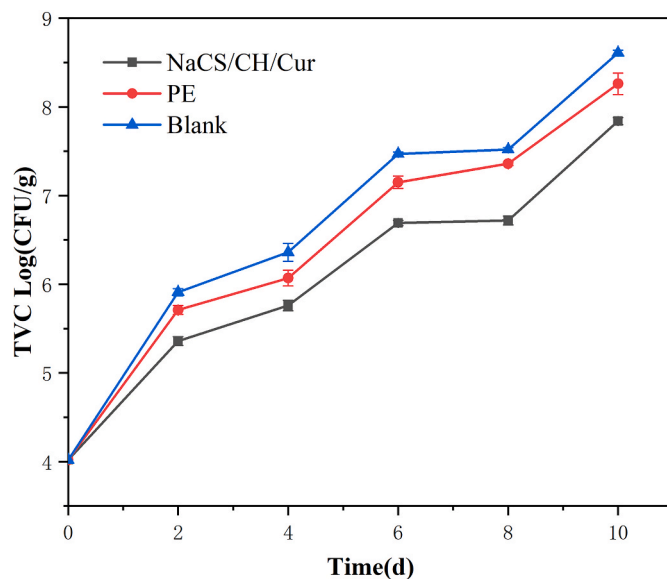


Fig. 7. Changes of TVC levels of pork. (NaCS/CH/Cur: wrapped pork with colorimetric film; PE: wrapped pork with polyethylene film; Blank: uncoated pork).

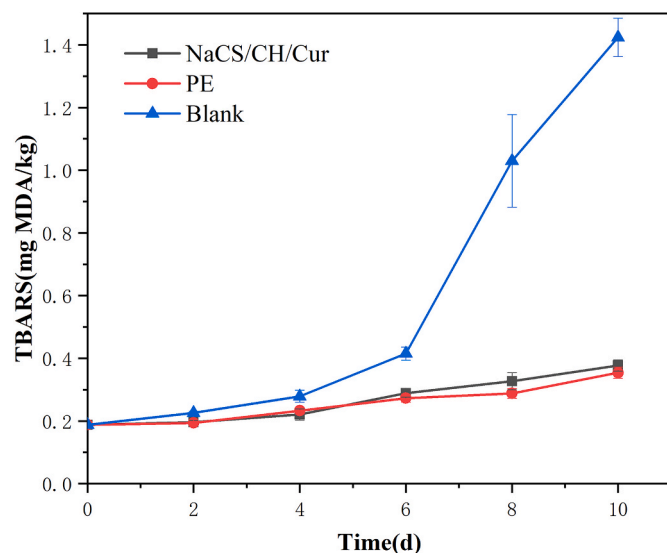







Fig. 8. Changes of TBARS levels of pork. (NaCS/CH/Cur: wrapped pork with colorimetric film; PE: wrapped pork with polyethylene film; Blank: uncoated pork).

was lower than that in the blank control. Chitosan showed very low antioxidant activity because CH lacks hydrogen atoms that could be easily donated (Schreiber et al., 2013). The antioxidant abilities of the composite films were mainly attributed to curcumin. Curcumin has a strong antioxidant capacity owing to its polyphenol structure (Xiao et al., 2021), which contains the phenoxy groups that can remove free radicals (Zhang et al., 2019). This study confirmed that both NaCS/CH/Cur composite films inhibited the oxidative rancidity of lipids.

The color parameters of the NaCS/CH/Cur films stored at 4 °C are listed in Table 3. After 6 days of storage, the TVB-N of the pork exceeded the limit, and the color of the colorimetric film changed. With the extension of the food storage time, L*, b*, and ΔE continued to increase, and a* decreased and then increased. The color of the NaCS/CH/Cur film changed significantly. The total color difference (ΔE) of the film

Table 3

The color parameters of the NaCS/CH/Cur film in contact with pork.

Time (day)	Photo	L*	a*	b*	ΔE
0		57.44 ± 0.27a	35.82 ± 1.10a	66.24 ± 0.53a	83.54 ± 0.87b
2		58.29 ± 0.99 ab	30.44 ± 1.50b	66.33 ± 0.65a	81.14 ± 0.30a
4		59.53 ± 0.34b	30.78 ± 0.74b	71.15 ± 0.62b	83.80 ± 0.54b
6		59.04 ± 0.86b	31.35 ± 0.44b	72.44 ± 0.62b	86.38 ± 0.47c
10		61.43 ± 1.05 ^c	31.77 ± 0.43 ^b	75.31 ± 0.35 ^c	88.21 ± 0.35 ^d

Means in the same column with different letters are statistically different ($p < 0.05$).

was 83.54, 86.38, and 88.21 at 0 day, 6th day, and 10th day of storage, respectively, suggesting that the color of the film changed significantly ($p < 0.05$). As shown in Table 3, the film was initially orange, changed to khaki on the 6th day, and turned yellow after the 10th day owing to the increase in pH. The film responded to the change in pH of pork, and the change in pH was induced by pork spoilage. Some researchers have prepared indicator films based on κ -carrageenan loaded with curcumin for monitoring pork at room temperature, and the results were highly consistent with ours (Liu et al., 2018). In conclusion, the NaCS/CH/Cur composite film can be used as an effective indicator for monitoring the freshness of animal protein-based foods.

4. Conclusions

NaCS/CH loaded with curcumin, as a pH-responsive colorimetric film, was prepared for intelligent food packaging. The mechanical properties and WVP test results showed that the NaCS/CH2:2 film had the highest TS and WVP values. It also had a higher TS and lower WVP after curcumin incorporation. The presence of curcumin enhanced the water vapor barrier and mechanical properties of the films. The SEM and FTIR results showed that curcumin was uniformly dispersed in the sodium cellulose sulfate/chitosan matrix. The colorimetric film exhibited a significant color change from yellow to red. For pork packaging, the color of the colorimetric film changed from orange to khaki, indicating that the fresh pork became spoiled. In addition, the colorimetric film showed stronger antibacterial activity than the PE packaging. Therefore, curcumin incorporated into sodium cellulose sulfate/chitosan film has a great potential in intelligent food packaging.

CRedit authorship contribution statement

Chuan Tang: Supervision, Funding acquisition, Project administration. **Zhixin Zhao:** Validation, Formal analysis, Writing – original draft. **Ming Yang:** Validation, Formal analysis, Writing – original draft. **Xuan Lu:** Formal analysis, Data curation. **Li Fu:** Visualization, Resources, Supervision. **Ge Jiang:** Supervision, Funding acquisition, Project administration.

Declaration of competing interest

The authors declare that they have no known competing financial interests or personal relationships that could have appeared to influence the work reported in this paper.

Acknowledgments

This work was supported by the National Natural Science Foundation of China (grant number 21606030), the Scientific Research Funding Project of the Education Department of Liaoning Province (grant number LJKZ1178), the Dalian High-level Talented Person Innovation

Support Plan Project (grant number 2019RQ118).

References

- Aggarwal, N., Altgärde, N., Svedhem, S., Zhang, K., Fischer, S., Groth, T., 2013. Effect of molecular composition of heparin and cellulose sulfate on multilayer formation and cell response. *Langmuir* 29 (45), 13853–13864. <https://doi.org/10.1021/la4028157>.
- Akyuz, L., Kaya, M., Koc, B., Mujtaba, M., Ilk, S., Labidi, J., Salaberria, A.M., Cakmak, Y. S., Yildiz, A., 2017. Diatomite as a novel composite ingredient for chitosan film with enhanced physicochemical properties. *Int. J. Biol. Macromol.* 105, 1401–1411. <https://doi.org/10.1016/j.ijbiomac.2017.08.161>.
- Chen, G., Zhang, B., Zhao, J., Chen, H.W., 2013. Improved process for the production of cellulose sulfate using sulfuric acid/ethanol solution. *Carbohydr. Polym.* 95 (1), 332–337. <https://doi.org/10.1016/j.carbpol.2013.03.003>.
- Chen, G., Liu, B., Zhang, B., 2014a. Characterization of composite hydrocolloid film based on sodium cellulose sulfate and cassava starch. *J. Food Eng.* 125, 105–111. <https://doi.org/10.1016/j.jfoodeng.2013.10.026>.
- Chen, G., Zhang, B., Zhao, Jun, Chen, H.W., 2014b. Development and characterization of food packaging film from cellulose sulfate. *Food Hydrocolloids* 35, 476–483. <https://doi.org/10.1016/j.foodhyd.2013.07.003>.
- Chen, H.L., Lan, G.Q., Ran, L.X., Xiao, Y., Yu, K., Lu, B.T., Dai, F.Y., Wu, D.Y., Lu, F., 2018. A novel wound dressing based on a Konjac glucomannan/silver nanoparticle composite sponge effectively kills bacteria and accelerates wound healing. *Carbohydr. Polym.* 183, 70–80. <https://doi.org/10.1016/j.carbpol.2017.11.029>.
- Chen, H.Z., Zhang, M., Bhandari, B., Yang, C.H., 2020. Novel pH-sensitive films containing curcumin and anthocyanins to monitor fish freshness. *Food Hydrocolloids* 100, 105438. <https://doi.org/10.1016/j.foodhyd.2019.105438>.
- Editorial Department of agricultural standards, 2015. *The Latest Agriculture Industry Standard China*. China Agricultural Press, Beijing.
- Ezati, P., Rhim, J.-W., 2019. pH-responsive pectin-based multifunctional films incorporated with curcumin and sulfur nanoparticles. *Carbohydr. Polym.* 230, 115638.
- Ezati, P., Rhim, J.-W., 2020. pH-responsive chitosan-based film incorporated with alizarin for intelligent packaging applications. *Food Hydrocolloids* 102, 105629. <https://doi.org/10.1016/j.foodhyd.2019.105629>.
- Huang, S., Xiong, Y., Zou, Y., Dong, Q., Ding, F., L., H.B., Liu, X., 2019. A novel colorimetric indicator based on agar incorporated with *Arnebia euchroma* root extracts for monitoring fish freshness. *Food Hydrocolloids* 90, 198–205. <https://doi.org/10.1016/j.foodhyd.2018.12.009>.
- Huang, J.Y., Chen, M.Y., Zhou, Y.Q., Li, Y., Hu, Y.Q., 2020. Functional characteristics improvement by structural modification of hydroxypropyl methylcellulose modified polyvinyl alcohol films incorporating roselle anthocyanins for shrimp freshness monitoring. *Int. J. Biol. Macromol.* 162, 1250–1261. <https://doi.org/10.1016/j.ijbiomac.2020.06.156>.
- Kadam, D., Momin, B., Palamthodi, S., Lele, S.S., 2019. Physicochemical and functional properties of chitosan-based nano-composite films incorporated with biogenic silver nanoparticles. *Carbohydr. Polym.* 211, 124–132. <https://doi.org/10.1016/j.carbpol.2019.02.005>.
- Kalkan, S., Otağ, M.R., Engin, M.S., 2020. Physicochemical and bioactive properties of edible methylcellulose films containing *rheum ribes* L. extract. *Food Chem.* 307, 125524. <https://doi.org/10.1016/j.foodchem.2019.125524>.
- Kang, S., Wang, H., Xia, L., Chen, M., Li, L., Cheng, J., Li, X., Jiang, S., 2020. Colorimetric film based on polyvinyl alcohol/okra mucilage polysaccharide incorporated with rose anthocyanins for shrimp freshness monitoring. *Carbohydr. Polym.* 229. <https://doi.org/10.1016/j.carbpol.2019.115402>. Article 115402.
- Kaur, S., Modi, N.H., Panda, D., Roy, N., 2010. Probing the binding site of curcumin in *Escherichia coli* and *Bacillus subtilis* PtsZ - a structural insight to unveil antibacterial activity of curcumin. *Eur. J. Med. Chem.* 45 (9), 4209–4214. <https://doi.org/10.1016/j.ejmech.2010.06.015>.
- Kim, D., Lee, S., Lee, K., Baek, S., Seo, J., 2017. Development of a pH indicator composed of high moisture-absorbing materials for real-time monitoring of chicken breast freshness. *Food Sci. Biotechnol.* 26 (1), 37–42. <https://doi.org/10.1007/s10068-017-0005-6>.
- Kurek, M., Garofulic, I.E., Bakic, M.T., Sctetar, M., Uzelac, V.D., Galic, K., 2018. Development and evaluation of a novel antioxidant and pH indicator film based on chitosan and food waste sources of antioxidants. *Food Hydrocolloids* 84, 238–246. <https://doi.org/10.1016/j.foodhyd.2018.05.050>.
- Liu, J.R., Wang, H.L., Wang, P.F., Guo, M., Jiang, S.W., Li, X.J., Jiang, S.T., 2018. Films based on κ -carrageenan incorporated with curcumin for freshness monitoring. *Food Hydrocolloids* 83, 134–142. <https://doi.org/10.1016/j.foodhyd.2018.05.012>.
- Liu, Y.H., Liu, M.Y., Zhang L., L., Cao Q., W., Wang, H., Chen R., G., Wang, S., 2022. Preparation and properties of biodegradable films made of cationic potato-peel starch and loaded with curcumin. *Food Hydrocolloids* 130, 107690. <https://doi.org/10.1016/j.foodhyd.2022.107690>.
- Liu, Y.T., Yuan, Y., Duan, S.Q., Li, C., Hu, B., Liu, A.P., Wu, D.T., Cui, H.Y., Lin, L., He, J. L., Wu, W.J., 2020. Preparation and characterization of chitosan films with three kinds of molecular weight for food packaging. *Int. J. Biol. Macromol.* 155, 249–259. <https://doi.org/10.1016/j.ijbiomac.2020.03.217>.
- Liu, Y.W., Ma, Y.L., Liu, Y., Zhang, J.L., Hossen, M., Sameen, M., Dai, J.W., Li, S.Q., Qin, W., 2022. Fabrication and characterization of pH-responsive intelligent films based on carboxymethyl cellulose and gelatin/curcumin/chitosan hybrid microcapsules for pork quality monitoring. *Food Hydrocolloids* 124, 107224. <https://doi.org/10.1016/j.foodhyd.2021.107224>.

- Medić, H., Kušec, I.D., Pleadin, J., Kozaciński, L., Niari, B., Hengl, B., Kušec, G., 2018. The impact of frozen storage duration on physical, chemical and microbiological properties of pork. *Meat Sci.* 140, 119–127. <https://doi.org/10.1016/j.meatsci.2018.03.006>.
- Medina-Jaramillo, C., Ochoa-Yepes, O., Bernal, C., Famá, L., 2017. Active and smart biodegradable packaging based on starch and natural extracts. *Carbohydr. Polym.* 176, 187–194. <https://doi.org/10.1016/j.carbpol.2017.08.079>.
- Muhtidinov, B., Heinze, T., Normakhamatov, N., Turayev, A., 2017. Preparation of sodium cellulose sulfate oligomers by free-radical depolymerization. *Carbohydr. Polym.* 173, 631–637. <https://doi.org/10.1016/j.carbpol.2017.06.033>.
- Pereda, M., Amica, G., Racz, I., Marcovich, N.E., 2011. Preparation and characterization of sodium caseinate films reinforced with cellulose derivatives. *Carbohydr. Polym.* 86, 1014–1021. <https://doi.org/10.1016/j.carbpol.2011.05.063>.
- Pirsa, S., Karimi Sani, I., Pirouzifard, M.K., Erfani, A., 2020. Smart film based on chitosan/Melissa officinalis essences/pomegranate peel extract to detect cream cheeses spoilage. *Food Addit. Contam.* 37 (4), 634–648. <https://doi.org/10.1080/19440049.2020.1716079>.
- Riaz, A., Lagnika, C., Luo, H., Nie, M., Dai, Z.Q., Liu, C.Q., Abidin, M., Hashim, M.M., Li, D.J., Song, J.F., 2020. Effect of Chinese chives (*Allium tuberosum*) addition to carboxymethyl cellulose based food packaging films. *Carbohydr. Polym.* 235, 115944 <https://doi.org/10.1016/j.carbpol.2020.115944>.
- Roy, S., Rhim, J.-W., 2020. Preparation of bioactive functional poly (lactic acid)/curcumin composite film for food packaging application. *Int. J. Biol. Macromol.* 162, 1780–1789. <https://doi.org/10.1016/j.ijbiomac.2020.08.094>.
- Schreiber, S.B., Bozell, J.J., Hayes, D.G., Zivanovic, S., 2013. Introduction of primary antioxidant activity to chitosan for application as a multifunctional food packaging material. *Food Hydrocolloids* 33 (2), 207–214. <https://doi.org/10.1016/j.foodhyd.2013.03.006>.
- Scordi-Bello, I.A., Mosoian, A., He, C., Chen, Y., Cheng, Y., Jarvis, G.A., Keller, M.J., Hogarty, K., Waller, D.P., Profy, A.T., Herold, B.C., Klotman, M.E., 2005. Candidate sulfonated and sulfated topical microbicides: comparison of anti-human immunodeficiency virus activities and mechanisms of action. *Antimicrob. Agents Chemother.* 49 (9), 3607–3615. <https://doi.org/10.1128/AAC.49.9.3607-3615.2005>.
- Shao, P., Liu, L., Yu, J., Lin, Y., Gao, H., Chen, H., Sun, P., 2021. An overview of intelligent freshness indicator packaging for food quality and safety monitoring. *Trends Food Sci. Technol.* 118, 285–296. <https://doi.org/10.1016/j.tifs.2021.10.012>.
- Sun, G.H., Chi, W.R., Xu, S.Y., Wang, L.J., 2020. Developing a simultaneously antioxidant and pH-responsive κ-carrageenan/hydroxypropyl methylcellulose film blended with *Prunus maackii* extract. *Int. J. Biol. Macromol.* 155, 1393–1400. <https://doi.org/10.1016/j.ijbiomac.2019.11.114>.
- Su, T., Wu, Q.X., Chen, Yan, Zha, Jin, Chen, X.D., Chen, J., 2019. Fabrication of the polyphosphates patched cellulose sulfate-chitosan hydrochloride microcapsules and as vehicles for sustained drug release. *Int. J. Pharm.* X 555, 291–302. <https://doi.org/10.1016/j.ijpharm.2018.11.058>.
- Wang, M.J., Xie, Y.L., Chen, Z.J., Yao, S.J., 2010. Optimizing preparation of NaCS-chitosan complex to form a potential material for the colon-specific drug delivery system. *J. Appl. Polym. Sci.* 117 (5), 3001–3012. <https://doi.org/10.1002/app.32259>.
- Wang, Y.J., Pan, M.H., Cheng, A.L., Lin, L.I., Ho, Y.S., Hsieh, C.Y., Lin, J.L., 1997. Stability of curcumin in buffer solutions and characterization of its degradation products. *J. Pharm. Biomed. Anal.* 15 (12), 1867–1876. [https://doi.org/10.1016/S0731-7085\(96\)02024-9](https://doi.org/10.1016/S0731-7085(96)02024-9).
- Wang, Z.M., Li, L., Zheng, B.S., Normakhamatov, N., Guo, S.Y., 2007. Preparation and anticoagulation activity of sodium cellulose sulfate. *Int. J. Biol. Macromol.* 41 (4), 376–382. <https://doi.org/10.1016/j.ijbiomac.2007.05.007>.
- Wu, C.H., Sun, J.S., Zheng, P.Y., Kang, X., Chen, M.Y., Li, Y.Z., Ge, Y.J., Hu, Y.Q., Pang, J., 2019. Preparation of an intelligent film based on chitosan/oxidized chitin nanocrystals incorporating black rice bran anthocyanins for seafood spoilage monitoring. *Carbohydr. Polym.* 222, 115006 <https://doi.org/10.1016/j.carbpol.2019.115006>.
- Wu, Q.X., Guan, Y.X., Yao, S.J., 2018. Sodium cellulose sulfate: a promising biomaterial used for microcarriers' designing. *Front. Chem. Sci. Eng.* 13 (1), 46–58. <https://doi.org/10.1007/s11705-018-1723-x>.
- Xiao, Y.Q., Liu, Y.N., Kang, S.F., Cui, M.D., Xu, H.D., 2021. Development of pH-responsive antioxidant soy protein isolate films incorporated with cellulose nanocrystals and curcumin nanocapsules to monitor shrimp freshness. *Food Hydrocolloids* 120, 106893. <https://doi.org/10.1016/j.foodhyd.2021.106893>.
- Yang, Y.N., Lu, K.Y., Wang, P., Ho, Y.C., Tsai, M.L., Mi, F.L., 2020. Development of bacterial cellulose/chitin multi-nanofibers based smart films containing natural active microspheres and nanoparticles formed in situ. *Carbohydr. Polym.* 228, 115370 <https://doi.org/10.1016/j.carbpol.2019.115370>.
- Yoshida, C.M.P., Maciel, V.B.V., Mendonca, M.E.D., Franco, T.T., 2014. Chitosan biobased and intelligent films: monitoring pH variations. *LWT—Food Sci. Technol.* 55, 83–89. <https://doi.org/10.1016/j.lwt.2013.09.015>.
- Yong, H.M., Liu, J., Qin, Y., Bai, R., Zhang, X., Liu, J., 2019. Antioxidant and pH-sensitive films developed by incorporating purple and black rice extracts into chitosan matrix. *Int. J. Biol. Macromol.* 137, 307–316. <https://doi.org/10.1016/j.ijbiomac.2019.07.009>.
- Zhai, X., Shi, J., Zou, X., Wang, S., Jiang, C., Zhang, J., Huang, X., Zhang, W., Holmes, M., 2017. Novel colorimetric films based on starch/polyvinyl alcohol incorporated with rosele anthocyanins for fish freshness monitoring. *Food Hydrocolloids* 69, 308–317. <https://doi.org/10.1016/j.foodhyd.2017.02.014>.
- Zhang, J.J., Zou, X.B., Zhai, X.D., Huang, X.W., Jiang, C.P., Holmes, M., 2019. Preparation of an intelligent pH film based on biodegradable polymers and rosele anthocyanins for monitoring pork freshness. *Food Chem.* 272, 306–312. <https://doi.org/10.1016/j.foodchem.2018.08.041>.
- Zhang, Q.L., Lin, D.Q., Yao, S.J., 2015. Review on biomedical and bioengineering applications of cellulose sulfate. *Carbohydr. Polym.* 132, 311–322. <https://doi.org/10.1016/j.carbpol.2015.06.041>.
- Zhao, S.S., Jia, R.Y., Yang, J., Dai, L., Ji, N., Xiong, L., Sun, Q.J., 2022. Development of chitosan/tannic acid/corn starch multifunctional bilayer smart films as pH-responsive actuators and for fruit preservation. *Int. J. Biol. Macromol.* 205, 419–429. <https://doi.org/10.1016/j.ijbiomac.2022.02.101>.
- Zhu, K.K., Shi, S., Cao, Y., Lu, A., Hu, J.L., Zhang, L.N., 2019. Robust chitin films with good biocompatibility and breathable properties. *Carbohydr. Polym.* 212, 361–367. <https://doi.org/10.1016/j.carbpol.2019.02.054>.
- Zhu, L.Y., Lin, D.Q., Yao, S.J., 2010. Biodegradation of polyelectrolyte complex films composed of chitosan and sodium cellulose sulfate as the controllable release carrier. *Carbohydr. Polym.* 82 (2), 323–328. <https://doi.org/10.1016/j.carbpol.2010.04.062>.
- Zimet, P., Mombrú, A.W., Mombrú, D., Castro, A., Villanueva, J.P., Pardo, H., Rufo, C., 2019. Physico-chemical and antilisterial properties of nisin-incorporated chitosan/carboxymethyl chitosan films. *Carbohydr. Polym.* 219 (1), 334–343. <https://doi.org/10.1016/j.carbpol.2019.05.013>.